Deletion of the Ca^{2+}-activated potassium (BK) α-subunit but not the BKβ1-subunit leads to progressive hearing loss

Lukas Rüttiger*†, Matthias Sausbier†‡, Ulrike Zimmermann*, Harald Winter*, Claudia Braig*, Jutta Engel§, Martina Knirsch§, Claudia Arntz‡, Patricia Langer*, Bernhard Hirt*, Marcus Müller¶‖, Iris Köpschall*, Markus Pfister¶, Stefan Münkner§, Karin Rohbock*, Imke Pfaff*, Alfons Rüsch§**, Peter Ruth‡, and Marlies Knipper*††

*Department of Otorhinolaryngology, Tübingen Hearing Research Center, Molecular Neurobiology and ¶Molecular Genetics, University of Tübingen, Elfriede-Aulhorn-Strasse 5, D-72076 Tübingen, Germany; ‡Institute of Pharmacy, Department of Pharmacology and Toxicology, University of Tübingen, Auf der Morgenstelle 8, D-72076 Tübingen, Germany; §Institute of Physiology II and Department of Otorhinolaryngology, Tübingen Hearing Research Center, University of Tübingen, Gmelinstrasse 5, D-72076 Tübingen, Germany; and ‖Department of Physiology II, University of Frankfurt, Theodor-Stern-Kai 7, 60590 Frankfurt am Main, Germany

Edited by Ramon Latorre, Center for Scientific Studies, Valdivia, Chile, and approved July 20, 2004 (received for review April 14, 2004)

The large conductance voltage- and Ca^{2+}-activated potassium (BK) channel has been suggested to play an important role in the signal transduction process of cochlear inner hair cells. BK channels have been shown to be composed of the pore-forming α-subunit coexpressed with the auxiliary β1-subunit. Analyzing the hearing function and cochlear phenotype of BK channel α- (BK$\alpha^{-/-}$) and β1-subunit (BK$\beta1^{-/-}$) knockout mice, we demonstrate normal hearing function and cochlear structure of BK$\beta1^{-/-}$ mice. During the first 4 postnatal weeks also, BK$\alpha^{-/-}$ mice most surprisingly did not show any obvious hearing deficits. High-frequency hearing loss developed in BK$\alpha^{-/-}$ mice only from ≈8 weeks postnatally onward and was accompanied by a lack of distortion product otoacoustic emissions, suggesting outer hair cell (OHC) dysfunction. Hearing loss was linked to a loss of the KCNQ4 potassium channel in membranes of OHCs in the basal and midbasal cochlear turn, preceding hair cell degeneration and leading to a similar phenotype as elicited by pharmacologic blockade of KCNQ4 channels. Although the actual link between BK gene deletion, loss of KCNQ4 in OHCs, and OHC degeneration requires further investigation, data already suggest human BK-coding *slo1* gene mutation as a susceptibility factor for progressive deafness, similar to KCNQ4 potassium channel mutations.

cochlea | KCNQ4

Ca^{2+}-activated potassium (BK) channels are heterooctamers of four α- and four β-subunits. The pore-forming α-subunit (KCNMA1) is a member of the *slo* family of potassium channels (1), originally identified in *Drosophila* (2). Studies of BK channels from smooth muscle have identified an auxiliary β1-subunit (KCNMB1) whose presence in the channel complex confers an increased voltage and calcium sensitivity toward the pore-forming α-subunit (3).

In turtle and chick, there is evidence that differential splicing of the BK channel α-subunit in conjunction with a graded expression of the auxiliary β-subunit along the tonotopic axis provides the functional heterogeneity of BK channels that underlies electrical tuning (for review, see ref. 4).

In inner hair cells (IHCs) of the mammalian organ of Corti, the predominant K^+ conductance is a voltage- and Ca^{2+}-activated K^+ channel termed $I_{K,f}$ (5, 6). BK channel mRNA (7, 8) and protein expression (8) were shown in IHCs, indicating that $I_{K,f}$ flows through BK channels. The presumed physiological roles of BK channels are (*i*) a decrease of the membrane time constant even at the resting potential and (*ii*) fast repolarization of the receptor potential. Both contribute to phase-locked receptor potentials up to high sound frequencies (6). In addition to IHCs, BK type Ca^{2+}-activated K^+ conductances have been measured in OHCs (9) and in efferent fibers onto outer hair cells (OHCs) (10). The role of BKs in either OHCs or efferents is still controversially discussed (9).

Studying the expression of BK channel α-splice variants and β-isoforms in rat cochlea using *in situ* hybridization and PCR techniques revealed the strict coexpression of a minimal variant of the α-transcript with the β1-transcript (7), indicating a functional role for both BK subunits in the mammalian cochlea.

In the present study, we used BK$\alpha^{-/-}$ (11) and BK$\beta1^{-/-}$ (12) mouse mutants to analyze the function of these channel subunits for development of normal hearing. Besides hearing measurements, the phenotype of the cochlea was studied by using markers for efferent (13) and afferent fibers (14). The integrity of IHCs and OHCs in adult mice was evaluated by assessing the expression of KCNQ4 (15, 16). Expression of the postsynaptic Ca^{2+}-dependent potassium channel SK2, which transduces specific responses of efferent neurons to OHCs (17), and the motor protein prestin (18, 19) was examined to prove a normal OHC phenotype. The observed subcellular distribution of the inwardly rectifying potassium channel subunit Kir4.1 in Deiters cells and the stria vascularis (20) and $K_v3.1$ in the stria vascularis and spiral ligament (21) suggested normal Deiters cell and stria vascularis phenotypes. Although lack of BKβ1 subunits allowed the development of a normal hearing function, deletion of the BKα gene resulted in progressive high-frequency hearing loss between 4 and 8 weeks, associated with a loss of active cochlear mechanics and of KCNQ4 in OHCs of basal/midbasal cochlear turns, suggesting a previously undescribed role of the BK channel for maintenance of KCNQ4 channel expression and thereby regular OHC function.

Materials and Methods

Animals. Care and use of the animals and the experimental protocol were reviewed and approved by the animal welfare commissioner and the regional board for scientific animal experiments in Tübingen.

BK Channel-Deficient Mice. BK$\alpha^{-/-}$ 129svj inbred mice were generated as described (11) and bred by mating BK$\alpha^{+/-}$ mice at the

This paper was submitted directly (Track II) to the PNAS office.

Freely available online through the PNAS open access option.

Abbreviations: IHC, inner hair cell; OHC, outer hair cell; ABR, auditory brainstem responses; DPOAE, distortion products of the otoacoustic emissions; DAPI, 4′,6-diamidino-2-phenylindole; BK, Ca^{2+}-activated potassium; CSP, cysteine string protein; SPL, sound pressure level.

†L.R. and M.S. contributed equally to this work.

**Deceased February 21, 2002.

††To whom correspondence should be addressed. E-mail: marlies.knipper@uni-tuebingen.de.

www.pnas.org/cgi/doi/10.1073/pnas.0402660101

animal house of the Institute of Pharmacy, Department of Pharmacology and Toxicology, University of Tübingen. Between 4 and 18 weeks of age, BK$\alpha^{-/-}$ were repetitively tested for their hearing thresholds and compared with their WT litters. Four to six cochleae of WT and BK$\alpha^{-/-}$ of each age were prepared for histology. BK$\beta1^{-/-}$ mice of 129svj/C57B6 mixed background were kindly provided by Richard Aldrich (Howard Hughes Medical Institute, Stanford University; ref. 12) and bred in the animal facilities of the Hearing Research Center, University of Tübingen. As control animals for the experiments with the BK$\beta1^{-/-}$ mice, we used 12- and 30-week-old mice of a mixed 129svj/C57B6 strain.

Hearing Measurements. Anesthesia of animals, measurements of auditory brainstem responses (ABR), and distortion products of the otoacoustic emissions (DPOAE) were performed as described (22, 23).

Western Blot. Western Blot analysis from cochlea tissue was performed as described (24). The specifity of the KCNQ4 antibody was verified by preadsorbing the antibody with the antigenic peptide.

Immunocytochemistry. Cochleae were isolated, dissected, fixed, cryosectioned, and stained as described (16, 22, 23). Anti-BKα (polyclonal anti-rabbit, Alomone Labs, Jerusalem; APC-021) and anti-BKα polyclonal antibody, recently generated (25), were used with similar results. To generate antibodies against KCNQ4, two rabbits were immunized (Charles River Breeding Laboratories, Kisslegg, Germany) with synthetic peptides corresponding to the C-terminal domain (amino acids 682–695, QTLSISRSVSTNMD, GenBank accession no. AF105202) of human KCNQ4. We furthermore used the following antibodies: affinity-purified goat polyclonal anti-KCNQ4 (polyclonal anti-goat, sc-9385, Santa Cruz Biotechnology) and the appropriate antigenic peptide (sc-9385 P), anti-NF200 (polyclonal anti-sheep, The Binding Site, Heidelberg, Germany, PH187), anti-synaptophysin (polyclonal anti-sheep, The Binding Site, PH510), anti-cysteine string protein (CSP) (polyclonal anti-rabbit, Chemicon; AB1576), anti-prestin (18), anti-potassium channel SK2 (polyclonal anti-rabbit, Sigma, P0483), anti-Kir4.1 (polyclonal anti-rabbit, Alomone Labs; APC-035), and anti-K_v3.1b (polyclonal anti-rabbit, Alomone Labs; APC-014). Primary antibodies were detected with fluorescently labeled secondary IgG antibodies (Cy3-conjugated antibodies, Jackson ImmunoResearch Laboratories, West Grove, PA; and Alexa Fluor 488-conjugated antibodies, Molecular Probes). Sections were embedded [Vectashield with 4′,6-diamidino-2-phenylindole (DAPI), Vector Laboratories, Burlingame, CA] and photographed with epifluorescence illumination (Olympus, Melville, NY; AX70 microscope).

For hematoxylin/eosin staining, cochleae were thawed and stained for 5 min (Mayers Hemalaun solution, Carl Roth, Karlsruhe, Germany), rinsed 10 min with running water, washed in distilled water, stained 7 min (0.1% eosin G solution in water), washed 5 min in distilled water, and embedded (Mowiol, Calbiochem–Novachem).

Laser Confocal Microscopy. Cochlea of WT mice (3 weeks) were fixed 30 min in 4% paraformaldehyde in PBS. The cochlear duct was prepared, segmented, and stained with rabbit anti-KCNQ4, rabbit anti-BK, and sheep anti-synaptophysin. Images were obtained by using a confocal laser-scanning microscope (Zeiss LSM 510), as described (16).

Terminal Deoxynucleotidyltransferase-Mediated dUTP Nick End Labeling and Caspase-3 Double Labeling. Detection of apoptosis was performed by using the *In Situ* Apoptosis Detection Kit (R&D Systems; TA4625), a caspase-3 antibody (polyclonal anti-rabbit, Cell Signaling Technology, Beverly, MA, #9661), and the Cell and Tissue Staining Kit (R&D Systems, CTS005).

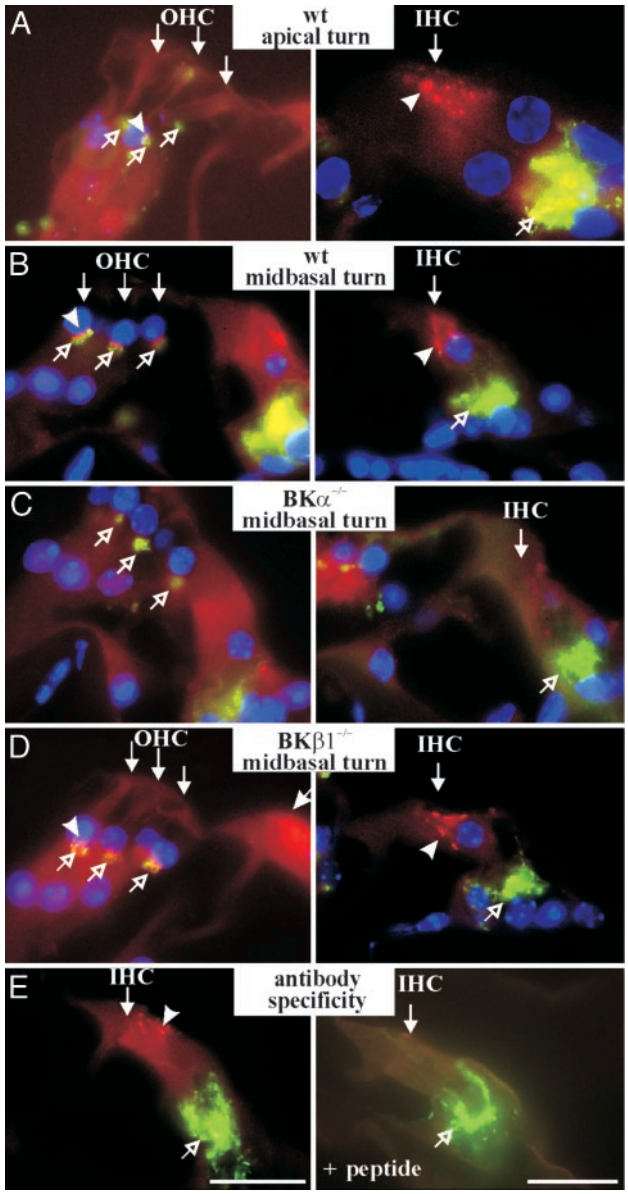

Fig. 1. Immunohistochemical localization of the BK channel α-subunit in the organ of Corti of WT (*A* and *B*), BK$\alpha^{-/-}$ (*C*), and BK$\beta1^{-/-}$ (*D*) mice using triple staining with anti-BKα (red), anti-synaptophysin (a marker for efferent boutons; green), and DAPI (a nuclear stain; blue). The experiment was replicated with similar result ($n > 20$). (*E*) Preadsorbing the BKα antibody with the antigenic peptide resulted in a complete absence of the immunoreaction. Filled arrows point to OHC and IHC, respectively. Open arrows point to the synaptic region of the hair cells, and arrowheads point to BKα-immunopositive staining. (Bar = 20 μm.)

Results

BK Channel Expression in the Cochlea of WT and Mutant Mice. The BKα-subunit was immunohistochemically analyzed in the cochleae of WT, BK$\alpha^{-/-}$, and BK$\beta1^{-/-}$ animals at the age of 3 weeks (Fig. 1) using double-labeling of anti-BKα (red) and anti-synaptophysin (green). With similar results, anti-BKα (11, 25) and anti-BKα (Alomone Labs, APC-021) were used. In both WT (Fig. 1 *A* and *B*) and BK$\beta1^{-/-}$ mice (Fig. 1*D*), the BKα

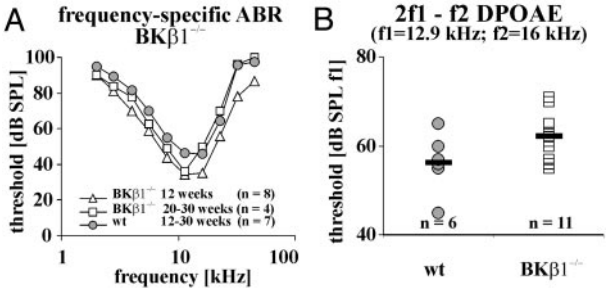

Fig. 2. ABR and DPOAE thresholds for WT and BK$\beta1^{-/-}$ mice. (*A*) ABR thresholds as a function of frequency for WT (circles) and BK$\beta1^{-/-}$ mice of 12 weeks (triangles) and 20–30 weeks (squares) of age. Standard deviations (not shown in graph for clarity reasons): WT, 10.8 (2.0–24.2); BK$\beta1^{-/-}$ 12 weeks, 9.6 (2.3–21.7); 20–30 weeks, 8.1 (2.5–16.8). (*B*) DPOAE thresholds (dB SPL f1) at f2 = 16 kHz for individual WT (circles) and BK$\beta1^{-/-}$ (squares) mice. Horizontal lines show the mean values.

protein was localized in the upper (supranuclear) part of IHCs (Fig. 1, IHC, arrowhead) and in close apposition to synaptophysin-immunopositive efferents to the OHCs (Fig. 1, OHC, open arrows). In BK$\alpha^{-/-}$ mice, BK staining was noted neither in IHCs nor OHCs (Fig. 1*C*). BK staining in OHCs but not in IHCs was reduced in apical turns (Fig. 1*A*) in analogy to a well described reduction of the number of efferent fibers toward more apical cochlear turns (26). Anti-BKα antibody specificity has been shown recently (11), and specificity for APC-021 anti-BKα was demonstrated by complete abolishment of immunostaining by preadsorbing the antibody with the peptide used for immunization, shown for IHC staining (Fig. 1*E*, antibody specificity).

Hearing Function in BK$\alpha^{-/-}$ and BK$\beta1^{-/-}$ Mice. ABR thresholds on click auditory stimuli were not different in WT [31.0 ± 11.1 dB sound pressure level (SPL), mean ± SD, $n = 10$] and BK$\beta1^{-/-}$ mice (25.6 ± 11.2 dB SPL, $n = 14$; $P > 0.05$). Frequency-specific ABR (Fig. 2*A*) and distortion product measurements (Fig. 2*B*) did not reveal any significant differences for WT and BK$\beta1^{-/-}$ mice for mean threshold and variance at all frequencies (Fig. 2*A*; mean: *t* test $P > 0.05$, SD: F test $P > 0.05$, n = 4–8). DPOAE thresholds as a function of f2 frequency of 16 kHz measured in WT (56.3 ± 6.6 dB SPL, $n = 6$), and BK$\beta1^{-/-}$ mutants (62.3 ± 5.3 dB SPL, $n = 11$) were without significant difference (Fig. 2*B*; $P > 0.05$). In line with the observed normal hearing function, whole cell recordings from IHCs of BK$\beta1^{-/-}$ mutants revealed normal BK current characteristics (D. Oliver, personal communication).

ABR thresholds to click stimuli in WT and BK$\alpha^{-/-}$ aged 4 weeks were similar (Fig. 3*A*; WT, 32.6 ± 10.1 dB SPL, $n = 9$; BK$\alpha^{-/-}$, 37.3 ± 9.0 dB SPL, $n = 8$; $P > 0.05$). A significant difference in the threshold, however, was observed when hearing function was tested in animals at 8 weeks of age (Fig. 3*B*; WT, 39.5 ± 9.7 dB SPL, $n = 4$; BK$\alpha^{-/-}$, 60.9 ± 7.5 dB SPL, $n = 4$; $P < 0.05$), and in animals aged 12–17 weeks (Fig. 3*C*; WT, 27.2 ± 8.7 dB SPL, $n = 9$; BK$\alpha^{-/-}$, 57.1 ± 13.9 dB SPL, $n = 13$; $P < 0.001$). The final threshold loss for click stimuli was ≈36 dB. The ABR thresholds for frequency-specific stimuli are shown in Fig. 3*D*. BK$\alpha^{-/-}$ at an age of 8–17 weeks had a significant threshold loss of 20–30 dB in the high frequency range >8 kHz (Fig. 3*D*; 11.3 kHz, $P < 0.05$; 16 kHz, $P < 0.001$; 22.63 kHz, $P < 0.001$; 32 kHz, $P > 0.05$). Threshold functions for WT animals were similar for all ages tested ($P > 0.05$) and did not show an age-related threshold loss or increase in variation (average SD, 14.5, 11.8, 13.9, and 14.6 for ages 4, 8, 12–14, and 17 weeks, respectively; F test $P > 0.05$).

DPOAE thresholds were measured as a function of f2 frequency of 16 kHz. Fig. 3*E* gives the numbers of ears where

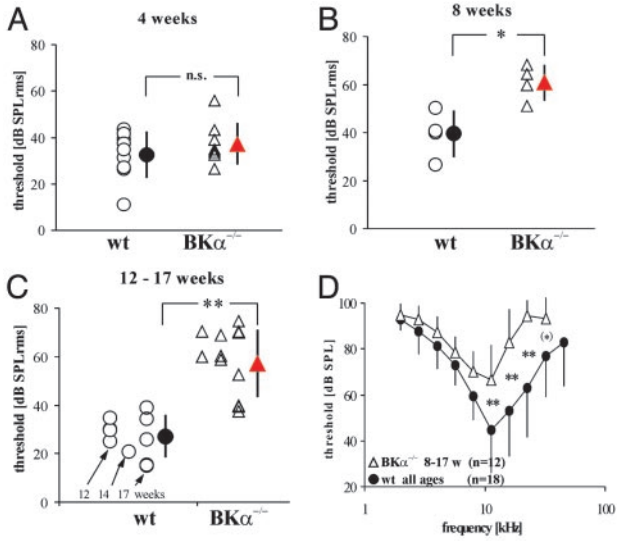

E

genotype	DPOAEs found	DPOAEs not found	number of ears
wildtype	10	10	20
heterzygote (+/–)	4	0	4
ko (–/–)	0	17	17
number of ears	14	27	41

Fig. 3. ABR thresholds of WT (circles) and BK$\alpha^{-/-}$ mice (triangles) (*A–D*) and number of ears with DPOAEs found (*E*). (*A–C*) ABR thresholds (dB SPL_{rms}) to click stimuli, given for individual mice (open symbols) and as mean (filled symbols) ± standard deviation as a function of age (*A*, 4 weeks; *B*, 8 weeks; *C*, 12–17 weeks). (*D*) ABR thresholds as a function of stimulus frequency for WT (circles) and BK$\alpha^{-/-}$ (triangles) mice of 8–17 weeks of age. (*E*) Number of ears with DPOAEs found. DPOAE function below 10 dB SPL could not be detected due to limitations of the method.

DPOAEs could be reported. In 10 of 20 WT and 4 of 4 BK$\alpha^{+/-}$ ears, DPOAEs were found. With our methods for measuring DPOAEs, significantly, DPOAEs could be found in none of the BK$\alpha^{-/-}$ mice tested ($n = 17$), independent of age (χ^2 test, $P < 0.05$).

Structural Evaluation of the Organ of Corti of BK Channel-Deficient Mice. The organ of Corti of WT mice (Fig. 4*A*) and BK$\beta1^{-/-}$ mice (Fig. 4*B*) did not show any difference in animals aged 14 weeks when stained with hematoxylin/eosin. In contrast, in BK$\alpha^{-/-}$ animals of the same age, when significant hearing loss was already noted, a severe degeneration of OHCs could be observed in the basal and midbasal cochlear turns (Fig. 4*C*, OHC), whereas we could not detect any noticeable changes in the IHC structure at that time (Fig. 4*C*, IHC).

The loss of OHCs at this age was accompanied by a detectable fragmentation of DNA and appearance of caspase-3 in Deiters cells (Fig. 4 *D* and *E*, open arrows). No signs of apoptosis were noted in the same sections in the stria vascularis and spiral ligament (data not shown).

Phenotype of the Cochlea at the Onset of Hearing Loss. Using Kir4.1 (20) and $K_v3.1$ (21) as markers for a presumptive normal phenotype of stria vascularis or spiral ligament fibrocytes, we were unable to detect alterations of the expression patterns in BK$\alpha^{-/-}$ mice in comparison to WT mice within the time period analyzed (data not shown).

Using CSP, which labels IHCs and efferent synapses (27), we could not detect any significant difference in IHC CSP expression in 4-, 8-, or 14-week-old WT and BK$\alpha^{-/-}$ mice (Fig. 5, IHC,

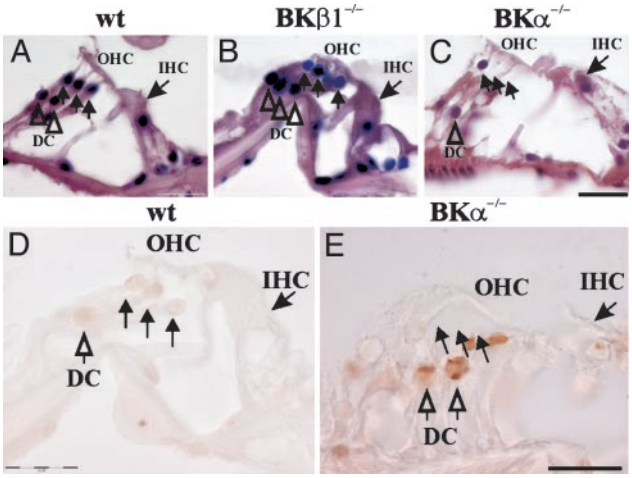

Fig. 4. Assessment of degenerative (*A–C*) and apoptotic (*D* and *E*) processes in the organ of Corti of WT, BK$\beta1^{-/-}$, and BK$\alpha^{-/-}$ mice at the age of 14 weeks. (*A–C*) Hematoxylin/eosin staining reveals morphological integrity of the midbasal cochlear turn in WT (*A*) and BK$\beta1^{-/-}$ (*B*) mice compared with severe degeneration of OHCs in BK$\alpha^{-/-}$ animals (*C*). (*D* and *E*) Double labeling of DNA fragmentation (terminal deoxynucleotidyltransferase-mediated dUTP nick end labeling staining) and caspase-3 immunoreactivity as a marker for apoptosis. Filled arrows depict three rows of OHCs and the IHC; open arrows depict Deiters cells. (Bar = 20 μm.)

4 and 14 weeks). Also, the expression of KCNQ4 and $Ca_v1.3$ in isolated IHCs of hearing-impaired BK$\alpha^{-/-}$ mice up to 14 weeks using RT-PCR was normal (data not shown). No differences in CSP expression were noted in efferent synapses below OHCs in normal hearing BK$\alpha^{-/-}$ mice at 4 weeks (Fig. 5, OHC), whereas CSP-immunopositive efferent synapses were absent in hearing-impaired BK$\alpha^{-/-}$ mice aged 14 weeks (Fig. 5, OHC). These results suggest a progressive degeneration of typical OHC phenotype causing the hearing deficit.

Next, we studied the influence of BKα deletion on the maintenance of the final phenotype of OHCs upon analyzing the expression of OHC ion channels such as KCNQ4, prestin, and SK2, or Kir4.1 channels expressed in the neighboring Deiters cells (20). Anti-KCNQ4 antibodies stained proteins at the OHC base (Fig. 6*A*), similar to the pattern described (15), and crossreacted with a corresponding polypeptide of ≈77 kDa in the absence but not presence of the antigenic peptide (Fig. 6*D*). Surprisingly, a loss of KCNQ4 in OHC membranes was noted

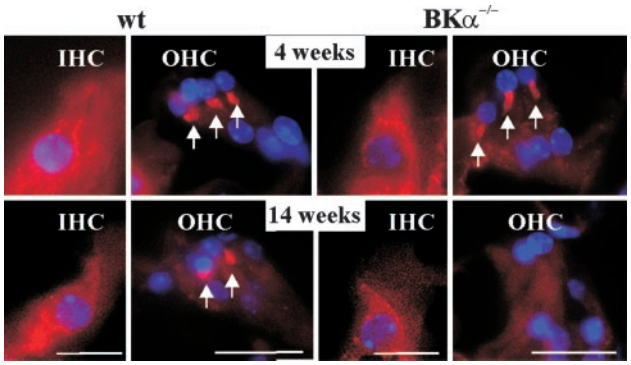

Fig. 5. Immunohistochemical assessment of the phenotype of the organ of Corti by using the synaptic vesicle marker anti-CSP (red) and the nuclear stain DAPI (blue) in midbasal cochlear turns in WT and BK$\alpha^{-/-}$, 4 and 14 weeks. CSP staining is noted in IHCs and efferent synapses. Note the reduced CSP immunoreactivity at the OHC but not IHC level in BK$\alpha^{-/-}$ animals at 14 weeks. (Bar = 20 μm.)

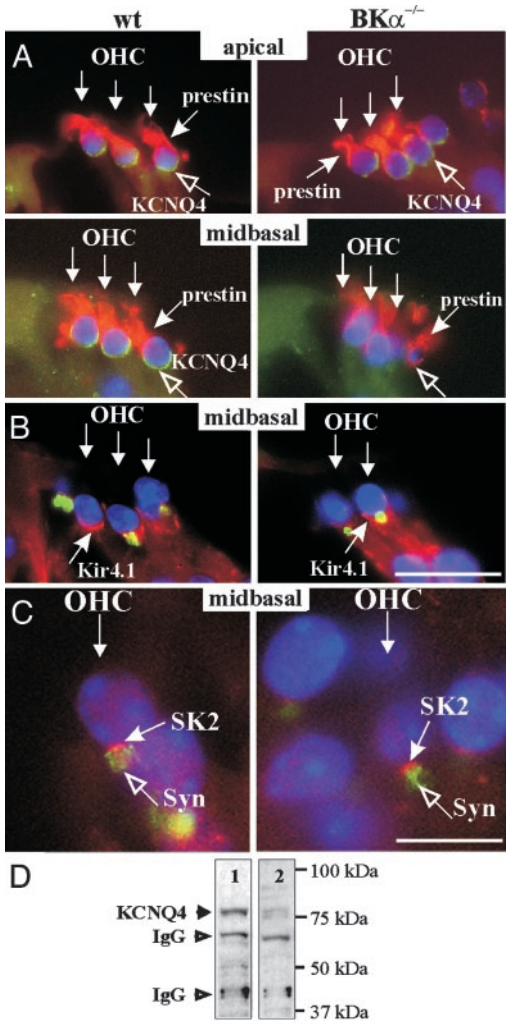

Fig. 6. Absence of KCNQ4 immunoreactivity in OHCs as a first indicator of loss of OHC phenotype. Cochlear sections of WT and BK$\alpha^{-/-}$ (8 weeks) of different turns were triple-stained for KCNQ4 (green), prestin (red), and DAPI (blue) (*A*); Kir4.1 (red), synaptophysin (green), and DAPI (blue) (*B*); and SK2 (red), synaptophysin (green), and DAPI (blue) (*C*). Note the decline of KCNQ4 in the midbasal but not apical cochlear turn in BK$\alpha^{-/-}$ mice, whereas prestin, synaptophysin, SK2, and Kir4.1 expression was still normal. (*D*) KCNQ4 antibody specificity was confirmed by detection of a band at the predicted molecular mass of ≈77 kDa in Western blot in membranes of cochlear tissue (lane 1) and the abolition of the 77-kDa Western signal by preadsorbing the antibody with the antigenic peptide (lane 2). (Bar in *A* and *B* = 50 μm; in *C* = 20 μm.)

before other overt signs of degeneration became evident. Three of six analyzed cochleae of 8-week-old BK$\alpha^{-/-}$ mice exhibited this early stage of degeneration shown in Fig. 6. At this time, BK$\alpha^{-/-}$ animals exhibited the exclusive loss of KCNQ4 proteins in OHCs of the basal and midbasal cochlear turns (Fig. 6*A*, midbasal, KCNQ4, open arrow) but not of the medial and apical cochlear turns (Fig. 6*A*, apical, open arrow). In the same cochlea, nearly all other proteins analyzed appeared to be normal, including prestin expression (Fig. 6*A*), Kir4.1 protein (Fig. 6*B*), synaptophysin-immunopositive efferent synaptic bodies (Fig. 6*C*, open arrow), and the postsynaptic SK2 channel protein (Fig. 6*C*, closed arrow).

Alteration of the Phenotype of the Cochlea During Hearing Loss. The degeneration process in OHCs of BK$\alpha^{-/-}$ mice subsequent to

CELL BIOLOGY

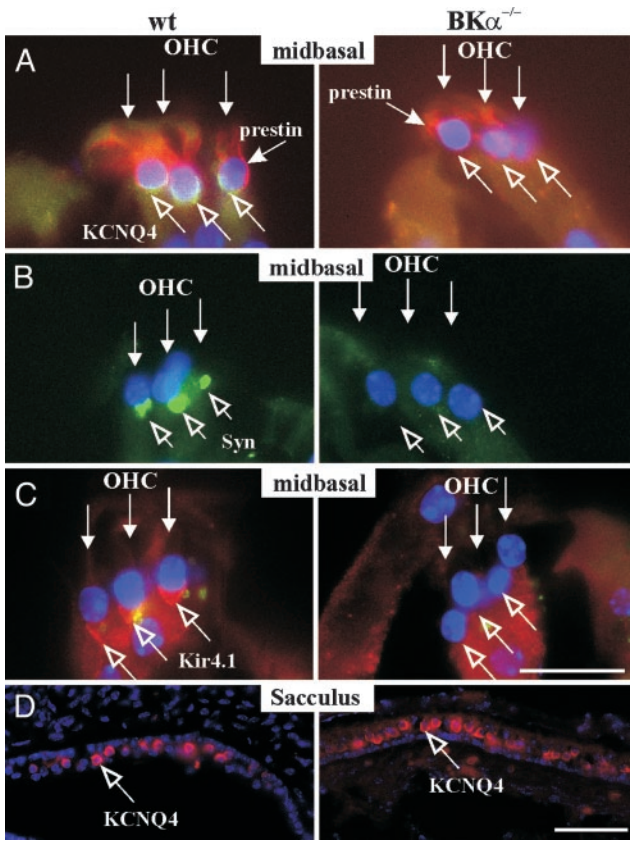

Fig. 7. Loss of OHC phenotype at 14 weeks of age. Midbasal cochlear sections of WT and BK$\alpha^{-/-}$ animals were triple-stained for prestin (red), KCNQ4 (green), and DAPI (blue) (*A*); double-stained for synaptophysin (green) and DAPI (blue) (*B*); and triple-stained for Kir4.1 (red), synaptophysin (green), and DAPI (blue) (*C*). (*D*) The vestibular organ (sacculus) was double-stained for KCNQ4 (red) and DAPI (blue). Note the loss of OHC phenotype in BK$\alpha^{-/-}$ mutants. (Bar = 20 μm.)

KCNQ4 loss, although appearing with a substantial variation over age, always occurred in the same sequence: (*i*) reduction of the size of efferent synaptic bodies, with a parallel reduction of the area of OHC membrane occupied by SK2 channels; (*ii*) disappearance of Kir4.1 from Deiters cells; (*iii*) complete loss of synaptophysin- or CSP-immunopositive efferents contacting the OHCs in basal and midbasal cochlear turns; and (*iv*) shrinkage of the membranes of OHCs with reduction of prestin protein.

Fig. 7 shows OHCs in a midbasal cochlear turn in WT and BK$\alpha^{-/-}$ at 14 weeks at a stage where simple light microscopy of OHCs would hardly reveal an alteration, and the staining of OHCs nuclei would suggest the existence of apparently normal OHCs (note the DAPI-stained OHC nuclei in Fig. 7 *A–C*). At this stage, a loss of KCNQ4 from OHC membranes was associated with a reduction of prestin protein in lateral membranes (Fig. 7*A*, KCNQ4, open arrows), the absence of synaptophysin-immunopositive boutons opposite OHCs (Fig. 7*B*, open arrows), and a complete vanishing of Kir4.1 from the apical Deiters cell membrane (Fig. 7*C*, open arrows). Normal KCNQ4 expression pattern was noted in the hair cells of the sacculus in the same cochlea (Fig. 7*D*).

Spatial Localization of BK Channels at OHCs. Laser confocal microscopy at the base of OHCs reveals a cup-form shape of KCNQ4 immunostaining shown from three different points of view (Fig. 8*A*, red) with a free spot, occupied by synaptophysin-immunopositive efferent boutons (Fig. 8*A*, green). Confocal

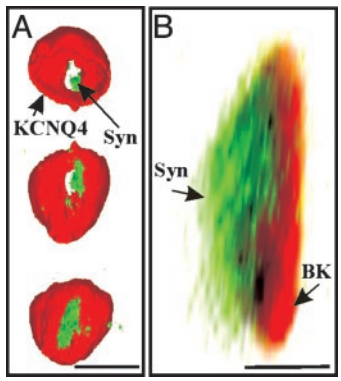

Fig. 8. Subcellular distribution of BK and KCNQ4 channels in OHCs. (*A*) 3D reconstruction of confocal image stacks of an OHC (whole-mount preparation, midbasal turn) stained for KCNQ4 (red) and synaptophysin (green). (*B*) 3D reconstruction of confocal image stacks of an OHC-efferent synapse (midbasal turn) stained for BK (red) and synaptopysin (green). Note that BK is localized at the postsynaptic side of the synaptopysin-immunopositive efferent presynapse. (Bar in *A* = 10 μm; in *B* = 2.5 μm.)

image stacks of the BK and synaptophysin-immunoreactive area at the OHC level in turn revealed the total spatial separation of both BK and synaptophysin staining patterns (Fig. 8*B*), demonstrating that the BK proteins are localized at the postsynaptic (OHC) side relative to the synaptophysin-immunopositive presynapse.

Discussion

Here, we show that mice lacking the BK channel pore-forming α-subunit apparently do not exhibit a congenital hearing loss, as would have been expected from the BK expression profile in IHC, but rather develop mild progressive high-frequency hearing loss, based on an alteration of the OHC phenotype. In contrast, mice lacking the auxiliary BK channel β1 gene do not exhibit any hearing deficits and have a normal cochlear phenotype. The data highlight unexpected previously undescribed functions of the BK channel complex for the inner ear.

BKβ1$^{-/-}$ Mice Have Normal Hearing and a Normal Cochlear Phenotype. In lower vertebrates, electrical tuning along the tonotopic axis is provided by differential BK channel expression (for review, see ref. 4). In the mammalian cochlea, however, tuning is based on the mechanical properties of the basilar membrane. Therefore, a role of the β1 subunit as a differential Ca^{2+} sensor is not to be expected in mammals. The data in the present study clearly indicate that BKβ1 plays no critical role for the normal basic hearing function. It cannot be excluded, however, that more intricate properties in the IHC transduction process are affected by the deletion of BKβ1 that could not be resolved with the techniques used.

BKα Deletion Leads to Hearing Loss Despite Normal Phenotypes of Stria Vascularis and Spiral Ligament. BK channels were shown to be present in the stria vascularis by immunocytochemistry (8) and electrophysiology (28) as well as in fibrocytes of the spiral ligament by electrophysiology (29). Although we cannot exclude effects on the endocochlear potential in BK$\alpha^{-/-}$ mice older than those studied here, we were unable to detect any phenotypical change in the stria vascularis in BK$\alpha^{-/-}$ mice, in line with the described profile of hearing loss.

BKα Deletion Leads to Hearing Loss Despite Inconspicuous IHC Phenotype. Kros *et al.* (6) argued that the BK current in IHCs is essential for a graded receptor potential and phase locking to frequencies in the kHz range. Whether phase locking was

affected by BKα gene deletion could not be answered due to the techniques used in this study. However, normal hearing function up to age 4 weeks indicates that graded receptor potentials are possible without BKα. Recently, evidence was presented for the presence of KCNQ4 channels in IHCs (16, 30). Although KCNQ4 provides a small maximum conductance, it is activated at the resting potential to $\approx$75%, which adds substantially to the total K^+ conductance around the resting potential, thereby contributing to a graded receptor potential. Expression of presynaptic elements of a normal IHC phenotype, such as CSP, a regulator of SNARE protein interactions (31), and $Ca_v1.3$ in BK$\alpha^{-/-}$ at least within the first 4 months underlines a probable normal IHC phenotype in the absence of BK. Future studies using conditional BKα gene deletion restricted to IHCs may exclude presumptive gene redundancy after embryonic gene deletion.

BKα Gene Deletion Leads to Hearing Loss Associated with OHC Degeneration. BK$\alpha^{-/-}$ mice develop high-frequency hearing loss and loss of DPOAEs after $\approx$2 months of age, concomitant with the first detectable sign of an altered cochlear phenotype, the disappearance of KCNQ4 from the OHC membranes in high-frequency regions of the cochlea.

The phenotype of KCNQ4$^{-/-}$ mice has not yet been described. However, a phenotype of mice after chronic block of KCNQ4 by linopirdine has been reported (32). The authors found a progressive loss of basal and midbasal but not apical OHCs, no influence on IHCs, reduced DPOAE amplitudes, and no effect on the endocochlear potential, indicating a normal stria vascularis, a nearly identical phenotype, as outlined here for the BK$\alpha^{-/-}$ mice. The striking similarity between the results of both studies leads to the conclusion that loss of KCNQ4 function in OHCs may lead to OHC degeneration. A possible explanation is that K^+ ions entering through the transduction channels lack a major exit route out of the OHCs, thus leading to chronic depolarization. The depolarization may cause induction of apoptosis via sustained Ca^{2+} influx through voltage-activated Ca^{2+} channels $Ca_v1.3$ (33). The depolarization also reduces the driving force that may explain the observed reduction in DPOAEs. Most interestingly in this context, KCNQ4 mutations (34) could be linked to hereditary deafness DFNA2 (35, 36), a hereditary disease that also results in progressive hearing loss for high-frequency sounds.

The distinct localization of BK channels opposite the efferent boutons (Fig. 8), occupying the same region as the SK2 channel (17), suggests a vital role of the BK current in the efferent inhibitory control. Whatever the function of BK on OHCs level, the similarity of basal to apical declining gradients of BK expression (present study) and the gradient of efferents (26) and presumptively afferent type II (22) indicates that BK channels play a role in maintaining those OHCs that receive efferent inhibitory feedback from the brain.

It will be a challenging topic of future research to uncover the series of events leading from BKα gene disruption to loss of KCNQ4 expression. But the data presented here already strongly suggest that human *slo1* must be considered an important susceptibility factor for progressive deafness analogous to KCNQ4 channel mutations (33).

This paper is dedicated to Alfons Rüsch. We thank Drs. Robert Brenner and Richard W. Aldrich (Department of Molecular and Cellular Physiology and Howard Hughes Medical Institute, Stanford University, Stanford, CA) for the generous supply of BKβ1 knockout mice. This work was supported by Deutsche Forschungsgemeinschaft Grants DFG Ru419, DFG Kni316/3-2, DFG Ru571/4-1, SFB 430-B3, and by Fortune 816-0-0.

1. Knaus, H. G., Garcia-Calvo, M., Kaczorowski, G. J. & Garcia, M. L. (1994) *J. Biol. Chem.* **269,** 3921–3924.
2. Elkins, T., Ganetzky, B. & Wu, C. F. (1986) *Proc. Natl. Acad. Sci. USA* **83,** 8415–8419.
3. McManus, O. B., Helms, L. M., Pallanck, L., Ganetzky, B., Swanson, R. & Leonard, R. J. (1995) *Neuron* **14,** 645–650.
4. Fettiplace, R. & Fuchs, P. A. (1999) *Annu. Rev. Physiol.* **61,** 809–834.
5. Dulon, D., Sugasawa, M., Blanchet, C. & Erostegui, C. (1995) *Pflügers Arch.* **430,** 365–373.
6. Kros, C. J., Ruppersberg, J. P. & Rusch, A. (1998) *Nature* **394,** 281–284.
7. Langer, P., Grunder, S. & Rusch, A. (2003) *J. Comp. Neurol.* **455,** 198–209.
8. Skinner, L. J., Enee, V., Beurg, M., Jung, H. H., Ryan, A. F., Hafidi, A., Aran, J. M. & Dulon, D. (2003) *J. Neurophysiol.* **90,** 320–332.
9. Mammano, F. & Ashmore, J. F. (1996) *J. Physiol.* **496,** 639–646.
10. Wangemann, P. & Takeuchi, S. (1993) *Hear. Res.* **66,** 123–129.
11. Sausbier, M., Hu, H., Arntz, C., Feil, S., Kamm, S., Adelsberger, H., Sausbier, U., Sailer, C. A., Feil, R., Hofmann, F., *et al.* (2004) *Proc. Natl. Acad. Sci. USA* **101,** 9474–9478.
12. Brenner, R., Jegla, T. J., Wickenden, A., Liu, Y. & Aldrich, R. W. (2000) *J. Biol. Chem.* **275,** 6453–6461.
13. Knipper, M., Zimmermann, U., Rohbock, K., Kopschall, I. & Zenner, H. P. (1995) *Brain Res. Dev. Brain Res.* **89,** 73–86.
14. Fermin, C. D., Martin, D. S. & Hara, H. (1997) *Cell Vis.* **4,** 280–297.
15. Kharkovets, T., Hardelin, J. P., Safieddine, S., Schweizer, M., El-Amraoui, A., Petit, C. & Jentsch, T. J. (2000) *Proc. Natl. Acad. Sci. USA* **97,** 4333–4338.
16. Oliver, D., Knipper, M., Derst, C. & Fakler, B. (2003) *J. Neurosci.* **23,** 2141–2149.
17. Oliver, D., Klocker, N., Schuck, J., Baukrowitz, T., Ruppersberg, J. P. & Fakler, B. (2000) *Neuron* **26,** 595–601.
18. Weber, T., Zimmermann, U., Winter, H., Mack, A., Kopschall, I., Rohbock, K., Zenner, H. P. & Knipper, M. (2002) *Proc. Natl. Acad. Sci. USA* **99,** 2901–2906.
19. Zheng, J., Shen, W., He, D. Z., Long, K. B., Madison, L. D. & Dallos, P. (2000) *Nature* **405,** 149–155.
20. Hibino, H., Horio, Y., Inanobe, A., Doi, K., Ito, M., Yamada, M., Gotow, T., Uchiyama, Y., Kawamura, M., Kubo, T. & Kurachi, Y. (1997) *J. Neurosci.* **17,** 4711–4721.
21. So, E., Kikuchi, T., Ishimaru, K., Miyabe, Y. & Kobayashi, T. (2001) *NeuroReport* **12,** 2761–2765.
22. Schimmang, T., Tan, J., Muller, M., Zimmermann, U., Rohbock, K., Kopschall, I., Limberger, A., Minichiello, L. & Knipper, M. (2003) *Development (Cambridge, U.K.)* **130,** 4741–4750.
23. Knipper, M., Zinn, C., Maier, H., Praetorius, M., Rohbock, K., Kopschall, I. & Zimmermann, U. (2000) *J. Neurophysiol.* **83,** 3101–3112.
24. Knipper, M., Richardson, G., Mack, A., Muller, M., Goodyear, R., Limberger, A., Rohbock, K., Kopschall, I., Zenner, H. P. & Zimmermann, U. (2001) *J. Biol. Chem.* **276,** 39046–39052.
25. Steffens, F., Zhou, X. B., Sausbier, U., Sailer, C., Motejlek, K., Ruth, P., Olcese, J., Korth, M. & Wieland, T. (2003) *Mol. Endocrinol.* **17,** 2103–2115.
26. Liberman, M. C. & Brown, M. C. (1986) *Hear. Res.* **24,** 17–36.
27. Eybalin, M., Renard, N., Aure, F. & Safieddine, S. (2002) *Eur. J. Neurosci.* **15,** 1409–1420.
28. Takeuchi, S., Marcus, D. C. & Wangemann, P. (1992) *Hear. Res.* **61,** 86–96.
29. Liang, F., Niedzielski, A., Schulte, B. A., Spicer, S. S., Hazen-Martin, D. J. & Shen, Z. (2003) *Pflügers Arch.* **445,** 683–692.
30. Marcotti, W., Johnson, S. L., Holley, M. C. & Kros, C. J. (2003) *J. Physiol.* **548,** 383–400.
31. Chamberlain, L. H. & Burgoyne, R. D. (2000) *J. Neurochem.* **74,** 1781–1789.
32. Nouvian, R., Ruel, J., Wang, J., Guitton, M. J., Pujol, R. & Puel, J. L. (2003) *Eur. J. Neurosci.* **17,** 2553–2562.
33. Michna, M., Knirsch, M., Hoda, J. C., Muenkner, S., Langer, P., Platzer, J., Striessnig, J. & Engel, J. (2003) *J. Physiol.* **553,** 747–758.
34. Kubisch, C., Schroeder, B. C., Friedrich, T., Lutjohann, B., El-Amraoui, A., Marlin, S., Petit, C. & Jentsch, T. J. (1999) *Cell* **96,** 437–446.
35. Coucke, P. J., Van Hauwe, P., Kelley, P. M., Kunst, H., Schatteman, I., Van Velzen, D., Meyers, J., Ensink, R. J., Verstreken, M., Declau, F., *et al.* (1999) *Hum. Mol. Genet.* **8,** 1321–1328.
36. Van Hauwe, P., Coucke, P. J., Ensink, R. J., Huygen, P., Cremers, C. W. & Van Camp, G. (2000) *Am. J. Med. Genet.* **93,** 184–187.